Perylene Polyether Hybrids: Highly Soluble, Luminescent, Redox-Active Dyes

Mary Elizabeth Williams and Royce W. Murray*

Kenan Laboratories of Chemistry, University of North Carolina, Chapel Hill, North Carolina 27599-3290

Received May 21, 1998. Revised Manuscript Received August 31, 1998

A new class of hybrid redox polyether melts has been prepared by covalent attachment of short polyethylene oxide "tails" to perylene, resulting in highly viscous materials with improved solubility in common solvents ranging from alcohols to toluene. Solid-state voltammetry of the neat, undiluted materials is made possible by dissolution of $LiClO_4$ supporting electrolyte in them. The perylene$^{0/1-}$ electron self-exchange rate constants (k_{EX}) are large. Temperature studies show that the energy barrier is also large but that the reactions are adiabatic. The ionic conductivity of the melts was measured to assess the effects of electron migration. The absorption and fluorescence properties of the perylene derivatives in dilute solution are independent of polyether tail length, while the fluorescence of thin undiluted films of the hybrids is red-shifted (relative to dilute solution) by ca. 125 nm and is dominated by excimer emission.

Introduction

Perylene and its tetracarboxylic acid derivatives are of interest as n-type molecular semiconductors,[1] as liquid crystals,[2] as dye sensitizers in solar cells,[3] in electrophotographic applications,[4] and as molecular components of light-emitting diodes.[5] These materials are attractive owing to their intense, high quantum yield fluorescence and general photostability, but suffer from poor solubilities in common solvents. Thin film perylenes are prepared by vapor deposition under high vacuum. It would be useful (in a processing sense) to be able to spin cast films.

Our interest in electron-transfer dynamics[6] and electrochemiluminescence[7] (ECL) in semisolid media has lead us to prepare a series of new perylene derivatives in which two oligomeric polyether chains (methyl end-capped "tails," MePEG, consisting of 3, 7, or 12 ethylene oxide monomer units, on average) are covalently linked to the perylene moiety via imide groups:

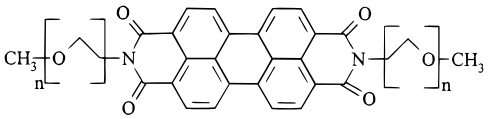

n = 3 ; **I**-E_3M
n = 7 ; **I**-350
n = 12 ; **I**-550

These structures (**I**) are abbreviated individually as **I**-E_3M, **I**-350, and **I**-550. The resulting "hybrid redox polyether" materials are from 0.7 to nearly 2 M in perylene centers,[8] and at room-temperature range with increasing tail length from (low melting) crystalline solids to viscous melts. The "melting" effect resulting from attaching the polyether chain is analogous to that experienced for several other redox systems.[6,7] Dissolving $LiClO_4$ in **I**-350 and **I**-550 renders them noncrystalline, slightly ionically conductive, and amenable to solid-state voltammetry experiments. We find that the rate constants for homogeneous electron self-exchange between the tailed perylene and its radical anion in the neat melts are comparable to the largest of those that we have observed in other electroactive hybrid redox polyether melts.[6,7]

(1) (a) Adams, D. M.; Kerimo, J.; Olson, E. J.; Zaban, A.; Gregg, B. A.; Barbara, P. F. *J. Am. Chem. Soc.* **1997**, *119*, 10608. (b) Horowitz, G.; Kouki, F.; Spearman, P.; Fichou, D.; Nogues, C.; Pan, X.; Garnier, F. *Adv. Mater.* **1996**, *8*, 242. (c) Meyer, J.-P.; Schlettwein, D.; Woehrle, D.; Jaeger, N. I. *Thin Solid Films* **1995**, *258*, 317. (d) Tanaka, K.; Nishio, S.; Matsuura, Y.; Yamabe, T. *Synth. Met.* **1993**, *55*, 896. (e) Tanaka, K.; Nishio, S.; Matsuura, Y.; Yamabe, T. *J. Appl. Phys.* **1993**, *73*, 5017.

(2) (a) Cormier, R. A.; Gregg, B. A. *Chem. Mater.* **1998**, *10*, 1309. (b) Cormier, R. A.; Gregg, B. A. *J. Phys. Chem. B.* **1997**, *101*, 11004.

(3) (a) Ferrere, S.; Zaban, A.; Gregg, B. A. *J. Phys. Chem. B.* **1997**, *101*, 4490. (b) Halls, J. J. M.; Friend, R. H. *Synth. Met.* **1997**, *85*, 1307. (c) Gregg, B. A. *Appl. Phys. Lett.* **1995**, *67*, 1271. (d) Whitlock, J. B.; Panayotatos, P.; Sharma, G. D.; Cox, M. D.; Sauers, R. R.; Bird, G. R. *Opt. Eng.* **1993**, *32*, 1921. (e) Siebentritt, S.; Guenster, S.; Meissner, D. *Synth. Met.* **1991**, *41*, 1173.

(4) Law, K. Y. *Chem. Rev.* **1993**, *93*, 449.

(5) (a) Hamm, S.; Wachtel, H. *J. Chem. Phys.* **1995**, *103*, 10689. (b) Toda, Y.; Yanagi, H. *Appl. Phys. Lett.* **1996**, *68*, 2315. (c) Kalinowski, J.; Di Marco, P.; Camaioni, M.; Fattori, V.; Stampor, W.; Duff, J. *Synth. Met.* **1996**, *76*, 77. (d) Burfeindt, B.; Hannappel, T.; Storck, W.; Willig, F. *J. Phys. Chem.* **1996**, *100*, 16463.

(6) (a) Long, J. W.; Kim, I. K.; Murray, R. W. *J. Am. Chem. Soc.* **1997**, *119*, 11510. (b) Williams, M. E.; Masui, H.; Long, J. W.; Malik, J.; Murray, R. W. *J. Am. Chem. Soc.* **1997**, *119*, 1997. (c) Williams, M. E.; Lyons, L. J.; Long, J. W.; Murray, R. W. *J. Phys. Chem. B.* **1997**, *101*, 7584. (d) Long, J. W.; Velasquez, C. S.; Murray, R. W. *J. Phys. Chem.* **1996**, *100*, 5492. (e) Terrill, R. H.; Hatazawa, T.; Murray, R. W. *J. Phys. Chem.* **1995**, *99*, 16676. (f) Hatazawa, T.; Terrill, R. H.; Murray, R. W. *Anal. Chem.* **1996**, *68*, 597.

(7) (a) Masui, H.; Murray, R. W. *Inorg. Chem.* **1997**, *36*, 5118. (b) Maness, K.; Masui, H.; Wightman, R. M.; Murray, R. W. *J. Am. Chem. Soc.* **1997**, *119*, 3987.

(8) (a) The measured densities of the melts are used to calculate the concentrations of perylene centers. (b) Equation 1 is for spherical reactants. For an anisotropic reactant (perylene) in an isotropic medium (the melt), the obtained k_{EX} is an average over relative reactant orientations and calculation of δ from concentration using a cubic lattice model is a reasonable approximation.

10.1021/cm980366z CCC: $15.00
Published on Web 10/09/1998

Table 1. Absorbance and Luminescence Data

complex	λ_{MAX}, nm (ϵ, M^{-1} cm^{-1})	λ_1, nm[a] (ϵ, M^{-1} cm^{-1})	λ_2, nm[a] (ϵ, M^{-1} cm^{-1})	$\lambda_{EM,MAX}$, nm	$\lambda_{EM,}$[a] nm	$\lambda_{EM2,}$[a] nm
I-E_3M (dilute solution)	526[b] (5.7×10^4)	490 (4.6×10^4)	458 (1.7×10^4)	540[e]	575	625
I-350 (dilute solution)	526[c] (6.1×10^4)	490 (4.6×10^4)	458 (1.8×10^4)	530[f]	580	630
I-550 (dilute solution)	524[d] (6.0×10^4)	488 (3.9×10^4)	458 (1.4×10^4)	538[g]	579	625
I-550 (neat film)[h]	480	554		655	~705	

[a] λ_1 and λ_2, and λ_{EM1} and λ_{EM2} denote wavelengths of the first and second satellites of the maximum absorbance and emission, respectively. [b] 5.3×10^{-5} M in CH_2Cl_2. [c] 3.6×10^{-5} M in $CHCl_3$. [d] 4.1×10^{-5} M in $CHCl_3$. [e] 1.6×10^{-6} M in CH_2Cl_2, excitation wavelength $\lambda_{EX} = 458$ nm. [f] 2.2×10^{-6} M in $CHCl_3$, $\lambda_{EX} = 480$ nm. [g] 1.3×10^{-6} M in $CHCl_3$, $\lambda_{EX} = 480$ nm. [h] Film thickness ca. 400 nm, on glass slide, spin-coated from CH_2Cl_2 solution.

The polyether chain additionally renders the perylene polyether hybrids quite soluble in a number of common solvents, enabling an examination of perylene dilute solution voltammetry, electronic spectroscopy, and electrochemiluminescence (ECL).

This paper reports the synthesis and early phase of our study of this new class of perylene materials, including the first example of voltammetry of a perylene as a pure material.

Results and Discussion

Absorbance and Luminescence of Dilute Solutions of I. The intense visible absorbance of perylene is well-known;[4] the perylene polyether hybrids **I** are also intensely colored. Figure 1A illustrates the normalized electronic absorbance (—) and luminescence (— —) spectra of **I**-550 in dilute chloroform solution. Table 1 summarizes the wavelength and molar absorptivities for the **I** derivatives, which are nearly identical with no apparent trend with polyether tail length. The well-defined vibronic progression in the absorbance and emission bands of **I** is typical of perylene derivatives and has been attributed to the symmetrical long-axis breathing mode of the perylene core.[9]

Figure 1B shows absorbance and emission spectra of a thin (ca. 400 nm) film of neat **I**-550; there are substantial differences between these and the dilute solution spectra. The vibronic detail is much less distinct in the solid-state spectrum. The central absorbance maximum in the pure **I**-550 film lies at roughly the same wavelength as the central vibronic band in dilute solution, but the lower energy absorbance of the band extends further into the red. The red color (vs black for thin films of strongly interacting perylene derivatives[10]) and absorbance spectrum of the neat material leads us to infer that the interactions between **I**-550 perylene cores are weak: the lack of interaction is presumably due to a longitudinal and translational offset from the common stacking of crystalline perylenes.[10]

The emission spectrum of neat **I**-550 (Figure 1B, - - -) is even more different from dilute solution; the emission λ_{MAX} is red-shifted by nearly 125 nm (Figure 1A, - - -). Similar shifts observed in the emission maxima of vapor-deposited perylene films having thicknesses of at least 2 monolayers have been attributed to excimer emission.[11] Continuing studies aim to more fully and quantitatively examine the apparent excimer formation in **I**, how it depends on the concentration of perylene sites, and various aspects of film casting and thermal annealing. Also of interest are the triplet relaxation spectra for the **I** derivatives, because of the possibilities for use as laser dyes as opened by the

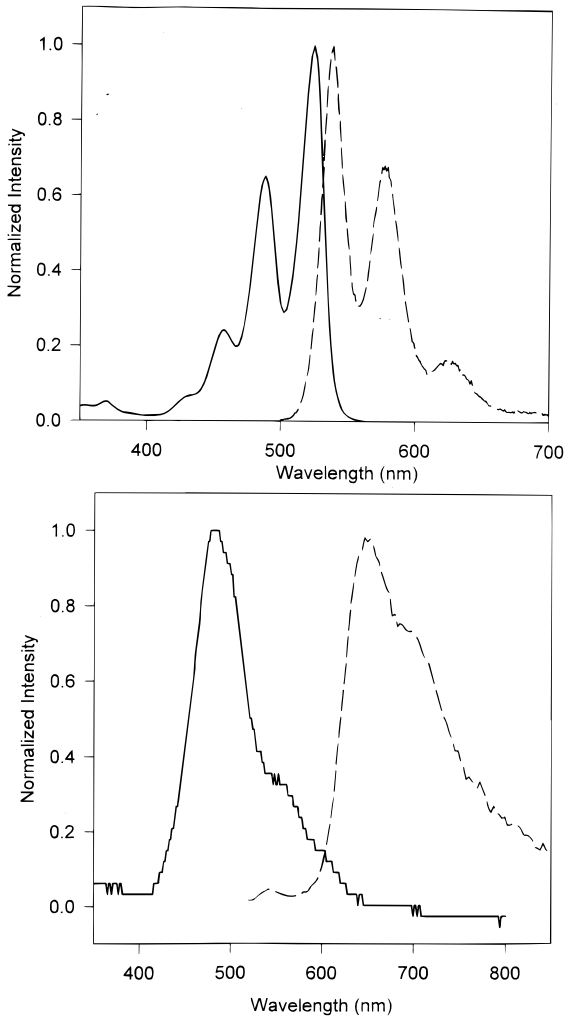

Figure 1. (A) Electronic absorbance and emission (excitation wavelength $\lambda_{EX} = 480$ nm) spectra of **I**-550 in $CHCl_3$. (B) Thin film (ca. 400 nm) absorbance and emission spectra of neat **I**-550 on glass, $\lambda_{EX} = 480$ nm.

(9) Sadrai, M.; Hadel, L.; Sauers, R..R.; Husain, S.; Krogh-Jesperson, K.; Westbrook, J. D.; Bird, G. R. *J. Phys. Chem.* **1992**, *96*, 7988.

(10) Kazmaier, P. M.; Hoffmann, R. *J. Am. Chem. Soc.* **1994**, *116*, 9684.

(11) Schlettwein, D.; Back, A.; Schilling, B.; Fritz, T.; Armstrong, N. R. *Chem. Mater.* **1998**, *10*, 601.

Table 2. Differential Scanning Calorimetry of Neat I

complex	T_G (°C)[a]	T_C (°C)[b]	T_M (°C)[c]
I-E_3M	−10	57	174
I-350	−75	*d*	*d*
I-550		−8	11
I-550/$LiClO_4$[e]	−39	*d*	*d*

[a] Apparent glass transition temperature determined from the average of the inflection points in heating and cooling curves. [b] Crystallization temperature, taken as the peak of the endothermic transition in the heating curve. [c] Melting temperature, taken as the peak of the exothermic transition in the heating curve. [d] No T_C or T_M observed. [e] **I**-550 melt containing 1.0 M $LiClO_4$.

alcohol and water-solubilizing effect of the polyether tails.

Solid State Electrochemistry of I-350 and I-550/$LiClO_4$. Previous microelectrode-based voltammetry in melts of hybrid redox polyethers has shown[6] that charge transport is (for most cases) dominated by electron diffusion (D_E, i.e., diffusion-like electron hopping or self-exchange) in the mixed valent layer generated at the electrode/melt interface. Physical diffusion (D_{PHYS}) of hybrid redox polyether sites tends to be very slow in their melts owing to the combination of large melt viscosity and the bulkiness of the diffusants. In fact, physical diffusion of the ClO_4^- electrolyte counterion can be faster than that of the hybrid redox polyether molecule itself.

The overall charge transport rate, or apparent diffusion coefficient (D_{APP}) is a summation of physical (D_{PHYS}) and electron (D_E) diffusion as described by the Dahms-Ruff equation:[12]

$$D_{APP} = D_{PHYS} + D_E = D_{PHYS} + \frac{k_{EX}\delta^2 C}{6} \qquad (1)$$

where k_{EX} is the electron self-exchange rate constant, δ the center-to-center reaction distance between redox sites, and C the redox site concentration.[8] On the basis of previous experiences,[6] we assume in this paper that D_{PHYS} in **I** is small relative to the electron hopping rate D_E, so that values of k_{EX} result directly from application of eq 1 to measured solid-state diffusivities, D_{APP}.

The MePEG tailed perylenes behave like other well-known polyethers[13] in that they readily dissolve $LiClO_4$ electrolyte by association of the Li^+ cation with the ether oxygens. We have shown previously[6a,14] that addition of $LiClO_4$ to neutral, polyether-tailed redox melts generates ionic conductivity sufficient to allow solid state (microelectrode) voltammetry. In this study, dissolution of $LiClO_4$ in **I**-550 additionally eliminates partial crystallinity of the polyether chains, rendering the material a viscous liquid (see DSC data in Table 2) with ionic conductivity sufficient for voltammetric measurement on the neat material.

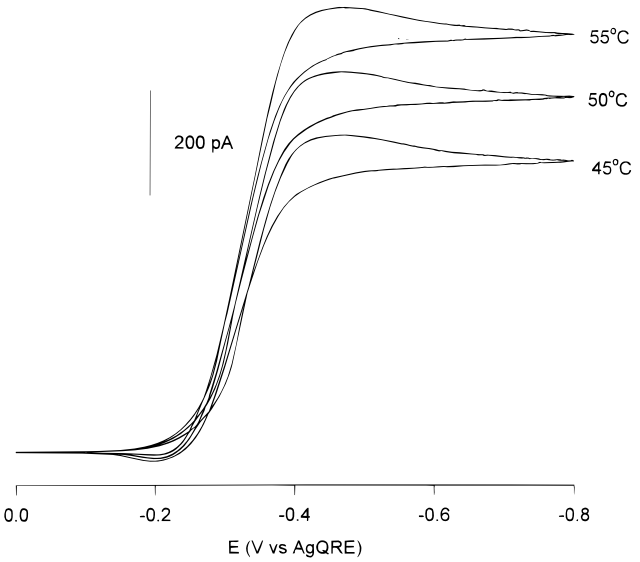

Figure 2. Solid-state cyclic voltammograms (2 mV/s) of **I**-550/$LiClO_4$ melt (O:Li 16:1) at a 2.6 μm diameter Pt microdisk working electrode at several temperatures.

Figure 2 shows the cyclic voltammetry at various temperatures of an **I**-550/$LiClO_4$ melt at a Pt microelectrode (2.6 μm diameter). (A single irreversible oxidation at ca. +1.8 V seen in the dry **I**-350/$LiClO_4$ and **I**-550/$LiClO_4$ films is not shown.) In contrast to the single wave in Figure 2, dilute solution voltammetry of **I** displays two reduction waves of equal size (vide infra). In the **I**-550/$LiClO_4$ and **I**-350/$LiClO_4$ (not shown) melts, the second reduction step appears to be strongly depressed and also shifted to slightly more negative potentials. The second reduction step is seen[15] in the **I**-350/$LiClO_4$ and **I**-550/$LiClO_4$ melts only in solvent-plasticized films, where it is much smaller than currents for the first reduction step. In completely dry **I**-350/$LiClO_4$ or **I**-550/$LiClO_4$ films (Figure 2), the second wave is not observed. The shift in formal potential for the second reduction, and the dramatic decrease in its current, may be associated with ionic migration and/or ion pairing effects, which have been observed[16] to a lesser degree in low ionic strength solutions. Given the possibilities for $(dimer)^{1-}$ formation in the neat perylene suggested by the luminescence spectra, the complete explanation may be even more complex.

The cyclic voltammograms in Figure 2 were taken at potential scan rates sufficiently slow as to achieve nearly steady-state diffusion. Faster potential scan voltammograms (not shown) result in mixed, linear-radial diffusion profiles that are convoluted by the effects of uncompensated resistance (iR_{UNC}). The apparent diffusion coefficient, D_{APP}, of the perylene$^{0/1-}$ reduction step was as a result most conveniently obtained from steady-state microdisk currents using the equation:

$$i_{SS} = 4nFrD_{APP}C \qquad (2)$$

(12) (a) Ruff, I.; Botar, L. *J. Chem. Phys.* **1985**, *83*, 1292. (b) Ruff, I.; Botar, L. *Chem. Phys. Lett.* **1986**, *126*, 348. (c) Ruff, I.; Botar, L. *Chem. Phys. Lett.* **1988**, *149*, 99. (d) Dahms, H. *J. Phys. Chem.* **1968**, *72*, 362. (e) Majda, M. In *Molecular Design of Electrode Surfaces*; Murray, R. W., Ed.; John Wiley & Sons: New York, 1992; p 159.

(13) (a) Grey, F. M. *Solid Polymer Electrolytes, Fundamentals and Technological Applications*; VCH Publishers: New York, 1992. (b) MacCallum, J. R.; Vincent, C. A. *Polymer Electrolyte Reviews*; Elsevier Applied Science: Oxford, UK, 1989; Vols. 1 and 2.

(14) Susan M. Hendrickson, University of North Carolina at Chapel Hill, unpublished results, 1998.

(15) Plasticization of the film with acetonitrile vapor enhances the current so that the second wave may be seen.

(16) (a) Amatore, C.; Paulson, S.; White, H. S. *J. Electroanal. Chem.* **1997**, *439*, 173. (b) Pletcher, D.; Thompson, H. *J. Chem. Soc., Faraday Trans.* **1997**, *93*, 3669. (c) Norton, J. D.; Benson, W. E. White, H. S.; Pendley, B. D.; Abruna, H. D. *Anal. Chem.* **1991**, *63*, 1909.

Table 3. Electron Self-Exchange Dynamics and Activation Results from Solid State Voltammetry of I-350/$LiClO_4$ and I-550/$LiClO_4$

	I-350[a]	**I**-550[b]
D_E (cm^2/s)[c] (25 °C)	1.2×10^{-9} [d]	3.1×10^{-9}
k_{EX} ($M^{-1}\ s^{-1}$)[c] (25 °C)	4.6×10^5	1.5×10^6
E_A (kJ mol^{-1})[e]	32	39
$k_{EX}{}^o$ ($M^{-1}\ s^{-1}$)[f]	2×10^{11}	1×10^{13}

[a] [**I**-350] = 1.1 M, average δ = 12 Å. [b] [**I**-550] = 0.70M, average δ = 13 Å. [c] Calculated from i_{SS} using eqs 1 and 2 assuming $D_{APP} \approx D_E$, then corrected for electronic migration effects (see the text). [d] The reported value of D_E is that extrapolated to 25 °C from a linear regression of the higher temperature Arrhenius plot for **I**-350/$LiClO_4$. Large uncompensated resistances prevented measurements of D_{APP} below 38 °C. [e] Activation energy obtained from the Arrhenius slope. [f] The intercept of the Arrhenius plot, $k_{EX}{}^o$, or $\kappa\nu$ according to eq 4 and ref 19.

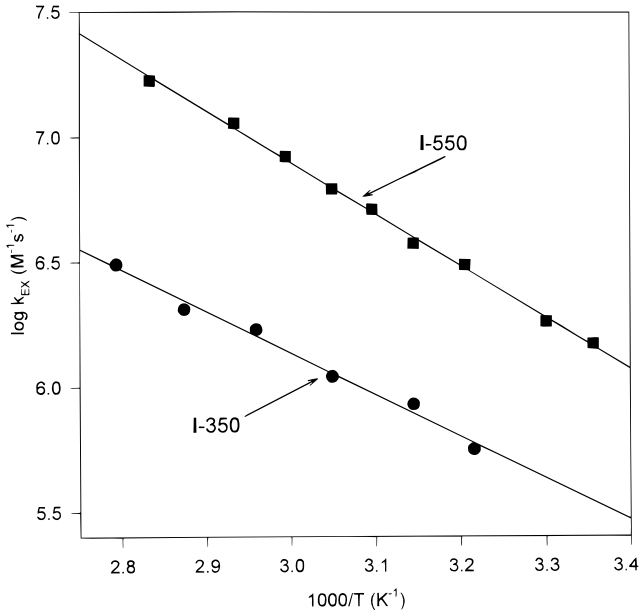

Figure 3. Activation plots of k_{EX} for **I**-350/$LiClO_4$ (●) and **I**-550/$LiClO_4$ (■) melts, with linear regressions (−).

where n is the number of electrons, F Faraday's constant, r the radius of the working electrode, and C the concentration of perylene redox sites. Steady-state currents were obtained either in slow potential scan cyclic voltammetry (as in Figure 2, ν < 1 mV/s) or from currents measured at long times (>300 s) after potential steps to the diffusion-limited plateau of the reduction. Table 3 gives resulting 25 °C values of D_E (corrected for electronic migration, vide infra) for **I**-350/$LiClO_4$ and **I**-550/$LiClO_4$ melts.

The electron self-exchange rate constants in Table 3 were calculated from eq 1 assuming that $D_{PHYS} \ll D_E$ and using a cubic lattice model to estimate δ.[8b] On the basis of previous results,[6] and considering the similarity of the viscosity properties of the polyether-tailed perylene to those of previously studied hybrid redox polyether melts, we believe this a reasonable assumption. The resulting values for k_{EX} are quite large (Table 3), indeed up to ca. 10-fold larger than those for metal-centered reactions in metal tris(bipyridine) and metalloporphyrin melts examined in previous studies.[6,14]

Figure 3 shows an Arrhenius plot of the rate constants k_{EX} from which we obtain (Table 3) an activation barrier energy, E_A, for the electron self-exchange based on

$$k_{EX} = A \exp(-E_A/RT) \tag{3}$$

which in contemporary terms is:[17]

$$k_{EX} = K_A \kappa\nu \exp\left[-\frac{\Delta G^*}{k_B T}\right] \tag{4}$$

where K_A is the precursor complex formation constant[18] for the donor−acceptor reaction pair, κ the transmission coefficient, ν the frequency factor, and $\Delta G^* \approx E_A$.[6b,17] The activation energy barriers for the **I**-350/$LiClO_4$ and **I**-550/$LiClO_4$ melts (Table 3) are not very different and are comparable to those found for polyether-tailed metal tris(bipyridine) and metalloporphyrin complexes.[6,7,14] Like the previous results, the perylene$^{0/1-}$ barriers are larger than predicted from dielectric continuum theory[19] for an "outer sphere" energy barrier in a conventional fluid ether solvent. The origin(s) of the enlarged barriers remain unclear. We suspect presently that effects associated with the dynamics of the polyether "solvent" that is covalently attached to the redox molecule are likely to be ultimately identified as contributors in part or whole.

The intercepts ($k_{EX}{}^o$) of the Arrhenius plots (Table 3; 10^{11} and 10^{13} $M^{-1}\ s^{-1}$ for the **I**-350/$LiClO_4$ and **I**-550/$LiClO_4$ melts, respectively) approach the vibrational limit of 10^{13}−10^{14} $M^{-1}\ s^{-1}$. When considered in the context of Marcus theory,[17] these values of $\kappa\nu$ imply that the reaction is an adiabatic electron transfer. This result rules out involvement of a large electron tunneling barrier provoked by an insulating shell of attached polyether. Aside from that point, the adiabatic result is unsurprising for electron transfers between a relatively rigid, multi-ring aromatic system and its structurally similar radical anion.

Ionic Conductivity. The ionic conductivities, σ_{IONIC}, of **I**-350/$LiClO_4$ and **I**-550/$LiClO_4$ melts were measured to probe melt ion mobilities and energetics and to assess the possible effects of migration on the electron transport rates (vide infra). The neat polyether-tailed perylenes, being neutral, have no intrinsic ionic conductivity, so the $LiClO_4$ electrolyte comprises the ionic charge-carrying capacity of the melt (at least before generation of perylene^{1-}). The measured σ_{IONIC} can be related to the mobility of the ions present using the Nernst−Einstein equation

$$\sigma_{IONIC} = \frac{F^2}{RT} \sum_i z_i{}^2 D_i C_i \tag{5}$$

where z_i and D_i are the charge on the ion and its physical diffusion coefficient, respectively. Because Li^+ associates strongly with the polyether oxygen, its mobility is constrained, and the melt ionic conductivity is assumed to arise mainly from the ClO_4^- anions. The ionic conductivity of the 25 °C melts and the calculated values of D_{ClO_4} are given in Table 4.[20] The ClO_4^- anions

(17) (a) Newton, M. D.; Sutin, N. *Annu. Rev. Phys. Chem.* **1984**, *35*, 437. (b) Marcus, R. A.; Sutin, N. *Biochim. Biophys. Acta* **1985**, *811*, 265. (c) Marcus, R. A.; Siddarth, P. In *Photoprocesses in Transition Metal Complexes, Biosystems, and Other Molecules*; Kochanski, E., Ed.; Kluwer Academic Publishers: Dordrecht, The Netherlands, 1992.

(18) The calculated value of K_A is ≈1 M^{-1} based on a concentration determined from density measurements.

(19) (a) Marcus, R. A. *Annu. Rev. Phys. Chem.* **1964**, *15*, 155. (b) Marcus, R. A. *J. Chem. Phys.* **1965**, *43*, 679.

Table 4. Ionic Conductivities of I-350/$LiClO_4$ and I-550/$LiClO_4$ Melts

	I-350	**I**-550
σ_{IONIC} (S/cm) (25 °C)	8.6×10^{-8}	9.0×10^{-7}
D_{ClO4} (cm^2/s) (25 °C)	2.2×10^{-11}	2.3×10^{-10}
$E_{A,IONIC}$ (kJ/mol)	52	54

[a] Calculated from eq 5 using $[ClO_4] = 1.0$ M.

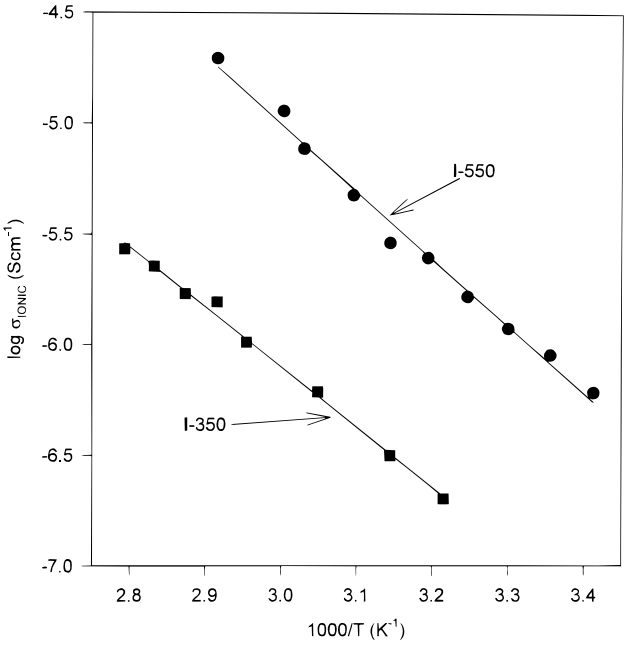

Figure 4. Activation plots of σ_{IONIC} for **I**-350/$LiClO_4$ (■) and **I**-550/$LiClO_4$ (●), with linear regressions (−).

are much smaller than the polyether-tailed perylene cores and are expected to be much more mobile; i.e. the physical diffusion (D_{PHYS}) rate of the tailed perylenes should be much smaller than D_{ClO_4}. Our assumption of $D_E \gg D_{PHYS}$ in the tailed perylene melts (above) is consistent with the Table 4 results for D_{ClO_4}, which in comparison to Table 3 show in turn that $D_E \gg D_{ClO_4}$.

Activation plots of σ_{IONIC} for **I**-350/$LiClO_4$ and **I**-550/$LiClO_4$ are shown in Figure 4; activation barrier energies for ionic conductivity, $E_{A,ION}$, are given in Table 4. The activation energy barrier for physical translation of the ClO_4^- anions is clearly much larger than that for charge translation by perylene$^{0/1-}$ electron self-exchange, which is analogous to previous results.[6a−c]

Effects of Electronic Migration. The measured ionic conductivities allow us to estimate the effects of electronic migration during voltammetry of the **I** melts. The melts can be approximated as fixed-site redox polymers in which the neutral, tailed perylene centers are relatively immobile (compared to the electrons). The Li^+ cations can also be thought of as "fixed-site" electroinactive ions (due to their strong association with the polyether oxygens), leaving the ClO_4^- anions to move in response to either concentration or electrical gradients. An electrical gradient forms during voltammetry, because the mobility (D_E, Table 3) of the electrons is greater than the mobility (D_{ClO_4},Table 4) of the ClO_4^- counterions, i.e., there is a substantial uncompensated resistance (iR_{UNC}) drop. The electrical gradient causes an acceleration of electron hopping rates.[21]

(20) This calculation assumes that $D_{Li} \ll D_{ClO_4}$ due to Li^+ association with the polyether chains.

Table 5. Dilute Solution Electrochemistry

complex	$E^{o\prime}_{0/1-}$ (V)[a]	$E^{o\prime}_{1-/2-}$ (V)[a]	$E_{a,peak,0/1+}$ (V)[a]
I-E_3M[b]	−0.68	−0.89	1.71
I-350[c]	−0.67	−0.86	1.62
I-550[d]	−0.74	−0.86	1.73

[a] Potentials are $E^{o\prime}$ vs SCE using Fc/Fc^+ as internal reference where Fc = ferrocene. [b] 0.5 mM in CH_2Cl_2, 0.1 M Bu_4NClO_4. [c] 0.5 mM in acetonitrile, 0.1 M Bu_4NClO_4. [d] 1 mM in acetonitrile, 0.1 M Bu_4NClO_4.

The values of D_E in Table 3 have been corrected[22] for electronic migration effects (as done previously[6b]); the correction lowers the raw D_E by factors of 1.5−4.5. The corrections involve the assumption that there is no ion pairing in the melts. If $Li^+ClO_4^-$ ion pairing occurs (which is in fact likely), the result is an *under*estimation of D_{ClO_4} and an *over*estimation of the electronic migration correction.[23] Because the extent of $Li^+ClO_4^-$ ion pairing in the melts is unknown, this leaves some uncertainty in the reported values. The electronic migration corrections also affect the barrier and intercepts, such that relative to the uncorrected results, E_A increases by 7 kJ/mol and k_{EX}^o by 10-fold for **I**-350, whereas for **I**-550, E_A increases by 5 kJ/mol and k_{EX}^o by a factor of 5. These are relatively minor effects. That is, the central interpretation of the electron hopping energetics remains unchanged; the reaction appears to be adiabatic and the activation barrier energy is much larger than explicable by an "outer sphere" model.

Dilute Solution Electrochemistry. Examination of the voltammetry of dilute solutions of the **I** polyether derivatives was made possible by their improved solubility. All three polyether-tailed materials exhibit two chemically reversible reduction waves (separated by ca. 120 mV) and a single, irreversible oxidation (at potentials close to the positive solvent breakdown limit) (Table 5). Figure 5 illustrates a reductive cyclic voltammogram of **I**-350 dissolved in CH_3CN. The two distinct voltammetric waves were observed during voltammetry over a wide range of concentrations of **I**, so the reductions do not appear to involve the formation of a dimeric species.

Solution Electrochemiluminescence. From fluorescence maxima (in Table 1), the difference between the perylene ground (S_0) and excited singlet state (S_1*) is ca. 2.3 eV. The perylene$^{0/1-}$ reduction potential allows calculation of the oxidation potential of a cation radical acceptor (A), whose reaction with perylene radical anion would be energetically capable of generating the excited singlet state. That is, to be energy sufficient to produce singlet electrochemiluminescence, an oxidation reaction by a species (A) with potential at least 2.3 V positive of the first perylene reduction wave is required, so that the following sequence can occur:

(21) Andrieux, C. P.; Saveant, J.-M. *J. Phys. Chem.* **1988**, *92*, 6761.

(22) The correction is based on working curves in ref 19 and has been used in previous work.[5] (a) **I**-350/$LiClO_4$: $\gamma = 0$, $n/z_C = -1$. (b) **I**-550/$LiClO_4$: $\gamma = 0.3$, $n/z_C = -1$.

(23) For example, assuming that 90% of the ClO_4^- anions are ion-paired in the melt, **I**-550 at 25 °C produces a migration-corrected value of D_E of 4.2×10^{-9} cm^2 s^{-1}, which is only 30% larger than D_E values corrected assuming no ion pairing.

$$A - e^- \rightarrow A^{1+} \quad (6)$$

$$P + e^- \rightarrow P^{1-} \quad (7)$$

$$A^{1+} + P^{1-} \rightarrow A + P^* \quad (8)$$

$$P^* \rightarrow P + h\nu \quad (9)$$

While the luminescence characteristics of perylene are well-documented, there are few examples of its electrogenerated chemiluminescence (ECL) in solution, unsurprising given its poor solubility in traditional electrochemical solvents. An exception is a report of ECL of dilute perylene in a $AlCl_3$/DMPIC molten salt solution,[24] in which ECL was generated by pulsing the potential between the formal potentials of the oxidation and reduction waves of perylene (in this case, perylene is both A and P in the above equations).

In the present work, because the polyether perylene derivatives apparently do not have a stable radical cation, another oxidant source was needed to generate the excited-state perylene. We employed a method described by Bard and co-workers,[25] where persulfate anions ($S_2O_8^{2-}$) are reduced (together with the molecule of interest), giving the strongly oxidizing SO_4^-, which in the present case reacts with reduced perylene to give the excited state, presumably according to the reactions

$$P + e^- \rightarrow P^{1-} \quad (10)$$

$$S_2O_8^{2-} + e^- \rightarrow SO_4^- + SO_4^{2-} \quad (11)$$

$$P^- + SO_4^- \rightarrow P^* + SO_4^{2-} \quad (12)$$

$$P^* \rightarrow P + h\nu \quad (13)$$

Figure 6A shows a cyclic voltammogram of a dilute solution of **I**-550 in CH_3CN/H_2O (50/50 v/v) containing 10 mM $(NH_4)_2S_2O_8$. The $S_2O_8^{2-}$ renders the normally reversible **I**-550 reduction (Figure 6C) chemically irreversible, due to the above reaction sequence. Figure 6B shows that the currents in Figure 6A lead to ECL, which is observed with a photomultiplier tube (PMT) located within 5 cm of the working electrode surface. The PMT current was collected concurrently with the electrochemical current.

Parts A and B of Figure 7 show the current and PMT response, respectively, of a solution of **I**-550 containing $(NH_4)_2S_2O_8$, to a 2 s potential step to −0.9 V (vs Ag QRE) and back. The ECL emission rises rapidly at the onset of the pulse, rapidly decays to a near-steady value, and ceases shortly after the potential pulse ends. Figure 7C shows the current (−) and PMT (- - -) responses for a solution of the polyether perylene derivative alone. It is clear from Figures 6 and 7 that the $S_2O_8^{2-}$ is a required coreactant for ECL emission. Background potential steps in a $(NH_4)_2S_2O_8$ solution do not produce light. Additional studies of the solution and solid-state ECL reactions of perylene with other electron acceptor(s) are underway and will be reported separately.

(24) (a) Mamantov, G.; Sienerth, K. D.; Lee, C. W.; Coffield, J. E. *J. Electrochem. Soc.* **1992**, *139*, L58. (b) $AlCl_3$ = aluminum chloride, DMPIC = 1,2-dimethyl-3-propyl-1*H*-imidazolium chloride.

(25) (a) Richter, M. M.; Debad, J. D.; Striplin, D. R.; Crosby, G. A.; Bard, A. J. *Anal. Chem.* **1996**, *68*, 4370. (b) Richter, M. M.; Bard, A. J. *Anal. Chem.* **1996**, *68*, 2641. (c) Richards, T. C.; Bard, A. J. *Anal. Chem.* **1995**, *34*, 3140.

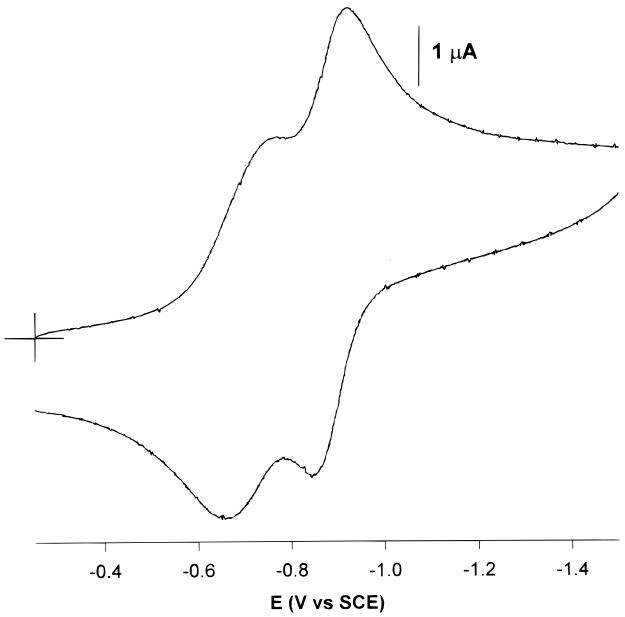

Figure 5. Dilute solution cyclic voltammetry (100 mV/s) of **I**-350 in acetonitrile with 0.1 M Bu_4NClO_4, with ferrocene$^{0/+}$ as internal reference, using a 1 cm diameter Pt working electrode.

Table 6. Solubility of Polyether Tailed Perylenes[a]

complex	H_2O	ethanol	acetone	CH_3CN	CH_2Cl_2	$CHCl_3$	toluene
I-E_3M	O	O	O	X	XX	XX	X
I-350	XX	X	X	XXX	XXX	XXX	X
I-550	XX	XX	XXX	XXX	XXX	XXX	XX

[a] O = insoluble; X = slightly soluble (<1 × 10^{-6} M); XX = soluble; XXX = very soluble (>10 mM).

Solubility. Perylene and 3,4,9,10-perylenetetracarboxylic acid dianhydride (PTCDA) are insoluble in most solvents. The latter dissolves only in strongly basic aqueous solutions, where the dianhydride groups are cleaved. Covalent attachment of polyether chains to PTCDA dramatically changes the solubility of the perylene center in common solvents and varies with polyether tail length. Table 6 lists rough solubilities in various solvents of the three polyether-tailed perylene derivatives. Others have seen improved solubility resulting from derivatization of the PTCDA core,[1−5] but those cases are limited to organic and chlorinated solvents.

The polyether-tailed derivatives dissolve easily in polar solvents. This is particularly helpful to solution voltammetry and ECL experiments, as well as to characterization by NMR, absorption, and fluorescence spectroscopies in conventional solvents.

Experimental Section

Chemicals. Triethylene oxide methyl ether (E_3M), poly(ethylene oxide) methyl ether (M_N = 350 g/mol, MePEG-350; M_N = 550 g/mol, MePEG-550) (Aldrich) were dried in a vacuum oven at 60 °C for a minimum of 24 h prior to use. *m*-Cresol and isoquinoline (Aldrich) were used as received. *p*-Toluenesulfonyl chloride (TosCl, Aldrich) was stored in a desiccator under nitrogen prior to use. Dimethylformamide (DMF) and acetonitrile (CH_3CN) were freshly distilled, dichloromethane (CH_2Cl_2) was dried over activated 4 Å molecular sieves, and other chemicals were used as received.

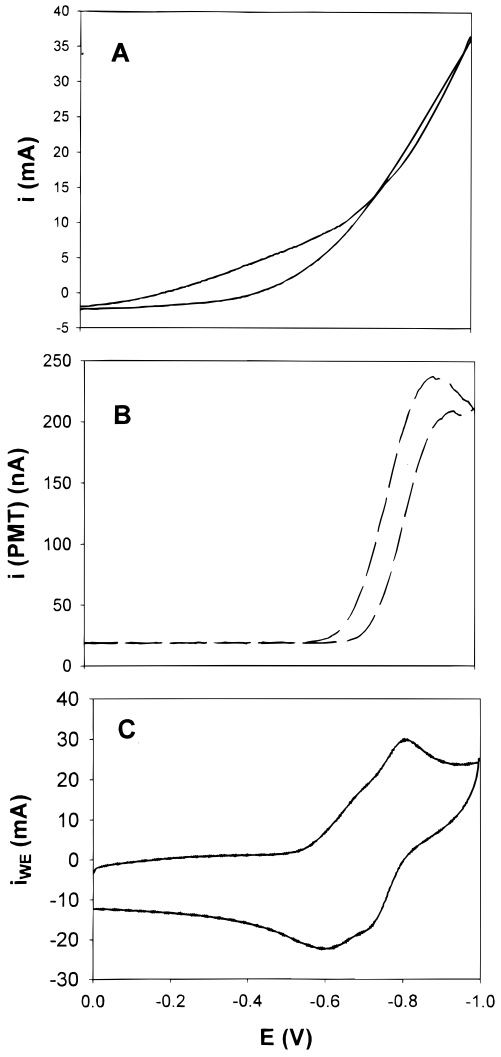

Figure 6. Dilute solution electrochemiluminescence of 1 mM **I**-550 in CH_3CN/H_2O (50/50 v/v) containing 0.1 M Bu_4NClO_4 and 10 mM $(NH_4)_2S_2O_8$. (A) Cyclic voltammogram (100 mV/s) using a 1 cm diameter Pt working electrode. (B) ECL emission collected simultaneously with panel A. (C) Cyclic voltammogram under the same conditions as A, but of a solution containing only **I**-550.

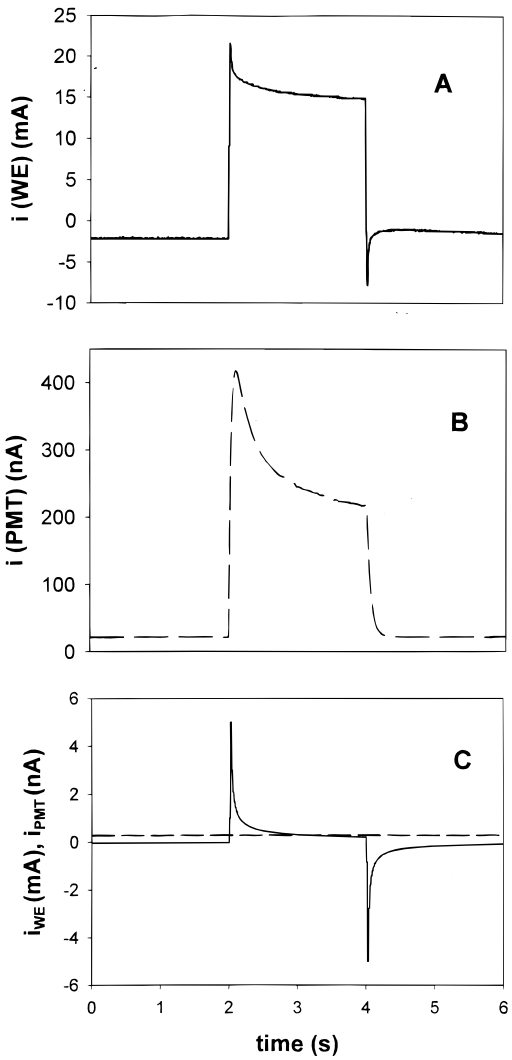

Figure 7. Solution ECL generated during a 2 s long potential step to −0.9 V at a 1 cm diameter Pt electrode. (A) Current for a solution of 1 mM **I**-550, 10 mM $(NH_4)_2S_2O_8$, 0.1 M Bu_4NClO_4 in CH_3CN/H_2O (50/50 v/v), and (B) PMT response collected simultaneously. (C) Background step for **I**-550 solution without $S_2O_8^{2-}$, where (- - -) is the PMT current and (−) is the working electrode current.

Analysis. UV−vis spectra were taken using a Unicam UV4 spectrometer. FTIR measurements were performed with a Bio-Rad FTS 6000 Spectrometer. Fluorescence emission spectra were taken using a Spex Fluorolog F212 emission spectrometer. Differential scanning calorimetry measurements were made with a Seiko DSC 220-CU at a heating/cooling rate of 10 °C/min, under nitrogen using thoroughly dried, preweighed samples. Elemental analysis was performed by Galbraith Laboratories, Knoxville, TN.

Electrochemical Measurements. Voltammetry was performed using a locally designed and constructed low-current potentiostat[26] with computer data acquisition and control. Dilute solutions were prepared using freshly distilled, thoroughly dried CH_3CN or CH_2Cl_2. The solutions were purged for at least 10 min with solvent-saturated nitrogen. Dilute solution voltammetry was done at a 1 cm diameter Pt disk working electrode with a Pt mesh counter electrode, Ag wire quasi-reference electrode, and ferrocene added to the solutions as an internal reference.

Solid-state voltammetry was executed as before[6,7] using a microdisk assembly containing the exposed tips of a 2.6 μm diameter Pt microdisk working electrode, a 24 gauge Pt counter electrode, and a 26 gauge Ag quasi-reference electrode. The assembly was polished with successively smaller grades of alumina (to 0.03 μm), rinsed with H_2O, and sonicated briefly in acetone. Perylene melt films (ca. 0.5 mm thick) were cast onto the assembly, such that contact was made among all three electrodes, and then dried under vacuum at 70 °C for 24 h. Temperature control was maintained with a Neslab Model RTE-140 circulating bath and measured using a thermocouple at the cell wall. All measurements were performed under vacuum, after the film had equilibrated to the desired temperature for a minimum of 1 h.

Ionic conductivities of the melts were measured under vacuum using AC impedance spectroscopy using a Solartron Model SI1260 Impedance Gain-Phase Analyzer with a SI1287 Electrochemical Interface. The electrode was a paired microband assembly containing two Pt microbands, each 1 cm long, 3 μm wide, and separated by 2 μm. A potential waveform with ac amplitude 20 mV, dc bias 0 V, and frequency range 100 kHz to 1 Hz was applied across the two electrodes. The intercept of the real axis in the complex impedance plot gives the bulk resistance, which is converted to ionic conductivity using the calibrated cell constant of the microband pair. Films were cast onto the electrodes from dilute solution in CH_3OH

(26) S. Woodward, University of North Carolina Chemistry Department Electronics Consultant.

and dried under vacuum at 70 °C for 24 h prior to measurement.

Light was collected during the ECL experiments with a Hamamatsu R5600U-01 photomultiplier tube (PMT) operated at 900 V using a Bertran Series 230 high-voltage power supply. The PMT current was amplified and converted to a voltage using a Stanford Research Systems SR570 low noise current preamplifier; input into a second channel on the same A/D board was used to collect the voltammetric signal.

Preparation of MePEG Amine. The same MePEG amine preparation procedure is used for the E_3M, MePEG-350, and MePEG-550 tails. The MePEGs are first tosylated according to a previously reported procedure.[6a] The MePEG-Tos is dried thoroughly in a vacuum oven at 70 °C for 24 h prior to use, and then 1 equiv is dissolved in DMF and stirred under nitrogen. An excess of NaN_3 (1.1 equiv) added to the solution immediately gives a tan suspension. The reaction mixture is heated to 100 °C for 6 h, giving a white precipitate in a tan solution. Cooling the mixture to room temperature and removing the solid by filtration and subsequently the solvent by rotary evaporation gives a yellow oil that is dried in the vacuum oven overnight. ^{1}H NMR confirms complete conversion to MePEG-N_3 reaction by the absence of the tosylate aromatic protons. FTIR confirms the presence of azide by the strong absorption at 2010 cm^{-1}. ^{1}H NMR (250 MHz) of MePEG-550-N_3 (for example) in $CDCl_3$: δ 3.7−3.5 (m, 48H), 3.32 (s, 3H).

Approximately 15 g of the dry MePEG-N_3 is dissolved in 50 mL of absolute ethanol and placed in a hydrogenation apparatus with 1.5 g Pd on carbon (10% Pd, Aldrich). The contents are purged for 10 min with nitrogen and then reacted under 30 psi of hydrogen at room-temperature overnight. The solution is purged with nitrogen to remove dissolved NH_3, the catalyst removed by vacuum filtration, and the ethanol removed on the rotary evaporator, giving a pale yellow, clear liquid. FTIR confirms complete conversion of the azide to amine by absence of the azide absorption and the presence of the amine bands above 3100 cm^{-1}.

Preparation of I Derivatives. A 0.25 g amount of pure, dry E_3M^- amine (1.6×10^{-3} mol) is combined with 0.30 g of 3,4,9,10-perylenetetracarboxylic acid dianhydride (PTCDA, Aldrich, 7.6×10^{-4}mol) in 30 mL of *m*-cresol and 3 mL of isoquinoline and reacted according to a literature procedure.[27] After cooling to room temperature, insoluble unreacted PTCDA is separated from the soluble product by filtration, and the solvents are removed by vacuum distillation, leaving a dark red solid residue. Acetone is used to suspend the solid, which is isolated by vacuum filtration, washed several times with acetone, and dried in a vacuum oven, giving the **I**-E_3M. ^{1}H NMR (200 MHz) in $CDCl_3$: δ 8.55 (d, 4H), 8.42 (d, 4H), 4.45 (t, 4H), 3.87 (t, 4H), 3.72 (m, 4H), 3.62 (m, 8H), 3.45 (m, 4H), 3.32 (s,6H).

Reaction of PTCDA with MePEG-350 amine is by the same procedure, except that after removal of the solvents, the residue is washed with diethyl ether several times (and allowed to stand overnight under Et_2O twice) to remove residual cresol and isoquinoline. The solvent is removed and the product dried in a vacuum oven, giving a dark red wax, **I**-350. ^{1}H NMR (200 MHz) in $CDCl_3$: δ 8.60 (m, 8H), 4.45 (t, 4H), 3.85 (t, 4H), 3.8−3.45 (m, 50H), 3.35 (s, 6H). Anal. calcd for $C_{53}H_{72}N_2O_{18}$: C, 62.5; O, 27.8; H, 6.9; N, 2.7. Found: C, 62.43, O, 28.18; H, 6.68; N, 2.91.

The MePEG-550-tailed molecule (**I**-550) is prepared analogously, giving a dark red wax. ^{1}H NMR (200 MHz) in $CDCl_3$: δ 8.62 (d, 4H), 8.55 (d, 4H), 4.45 (t, 4H), 3.85 (t, 4H), 3.7−3.5 (m, 85H), 3.32 (s, 6H). Anal. calcd for $C_{72}H_{108}N_2O_{27}$: C, 60.3; O, 30.2; H, 7.5; N, 1.9. Found: C, 59.58; O, 29.95; H 7.48; N 2.07.

Preparation of I-350/$LiClO_4$ and I-550/$LiClO_4$ Melts. The **I**-350 and **I**-550 are dried under vacuum at 80 °C for a minimum of 36 h and carefully weighed. An amount of $LiClO_4$ is added to the perylene such that the ratio of polyether oxygen to Li^+ cation is 16:1; there are 0.9 and 1.5 $LiClO_4$ for each **I**-350 and **I**-550, respectively. Sufficient acetone is added to completely dissolve both $LiClO_4$ and perylene, the solution stirred for 30 min, and the solvent removed by rotary evaporation. The resulting material is a viscous liquid and is used in its solvent-free form in the solid-state voltammetry experiments.

Acknowledgment. This work was supported in part by grants from the Department of Energy and the National Science Foundation. We are grateful to Prof. T. J. Meyer and co-workers for their assistance with the luminescence measurements. M.E.W. gratefully acknowledges receipt of a Summer Fellowship from the Electrochemical Society (1997) and the Albert G. Ledoux Fellowship from the University of North Carolina.

CM980366Z

(27) Icli, S.; Icil, H. *Spec. Lett.* **1996**, *29* (7), 1253.